

Inverse Design Guided Nanofabrication of Silicon Nitride Metasurface Structures for Wavelength Splitting

Muhammad Fasih^{1,2}, Abdulla Al Mamun^{1,2}, Eashan Chopde^{1,2}, Chao Wang^{1,2}

¹*School of Electrical Computer and Energy Engineering, Arizona State University, Tempe, AZ 85287 USA;*

²*Biodesign Center for Molecular Design and Biomimetics, Arizona State University, Tempe, AZ 85287 USA.*

Correspondence: wangch@asu.edu

Photonic wavelength splitters are key components in modern integrated photonic systems, enabling wavelength-selective signal processing for applications ranging from optical communications and spectroscopy to photonic sensing and biosensing. Conventional photonic designs rely on physics-based intuition and analytical models, which typically restrict achievable performance and footprint. To address these limitations, optimization-based inverse design methods, including topology optimization, have been widely explored to realize compact, non-intuitive nanophotonic structures with enhanced spectral selectivity^{1,2}. However, challenges remain in the fabrication robustness and manufacturability of such inverse-designed devices. In this work, we present the inverse design, fabrication, and experimental realization of a compact on-chip wavelength splitter operating in the visible to near-infrared range. Our approach employs a topology-optimization-driven inverse design framework, previously demonstrated primarily in the telecommunications wavelength regime (1300 nm, 1550 nm)¹, but here extended to the visible spectral range to enable integrated-photonics applications such as on-chip spectroscopy, optical sensing, and imaging, while incorporating fabrication-aware constraints and experimental nanofabrication validation. The spatial permittivity distribution within a confined design region is iteratively optimized to achieve wavelength-selective routing between multiple output waveguides, enabling systematic exploration of compact, high-performance geometries compatible with electron beam lithography (EBL).

Following design optimization, one testing structure was fabricated on a silicon substrate using standard cleanroom processes (Figure 3a). A silicon wafer was first coated with a silicon dioxide (SiO₂) undercladding deposited via plasma-enhanced chemical vapor deposition (PECVD), followed by thermal deposition of the silicon nitride (SiN) guiding layer. Nanostructure patterning was performed using high-resolution Elionix BODEN 100keV EBL tool with a bi-layer PMMA resist. A comprehensive dose calibration study was carried out using multiple exposure doses to systematically evaluate pattern fidelity, linewidth control, and feature resolution. From this dose matrix, an optimal exposure window was identified that reliably reproduces the inverse-designed features while minimizing line edge roughness and pattern collapse.

This work demonstrates a complete workflow spanning inverse electromagnetic design, process-aware optimization, and experimentally validated nanofabrication. Currently, complete device integration and characterization are ongoing and will be presented at the conference. Our approach provides a scalable pathway toward compact, integrated photonic wavelength devices for broad on-chip fluorescent imaging and spectroscopy applications.

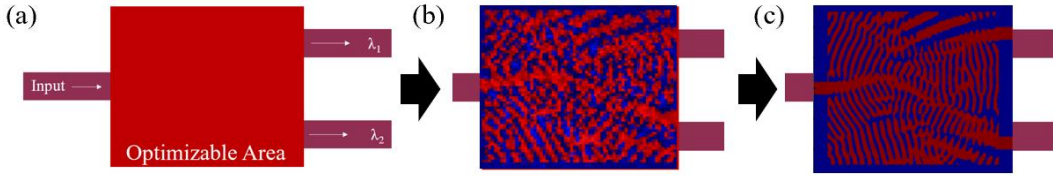


Figure 1: *Inverse design workflow for a wavelength-splitting device.*

(a) Initial design domain defining the optimizable region with a single input and two target output ports. (b) Intermediate stage, where the material permittivity is allowed to vary continuously between ϵ_{low} and ϵ_{high} , and is smoothly regularized using top-hat convolution to guide the optimization toward physically meaningful solutions. (c) Final optimized device geometry exhibiting well-defined structural features that enable wavelength-selective routing.

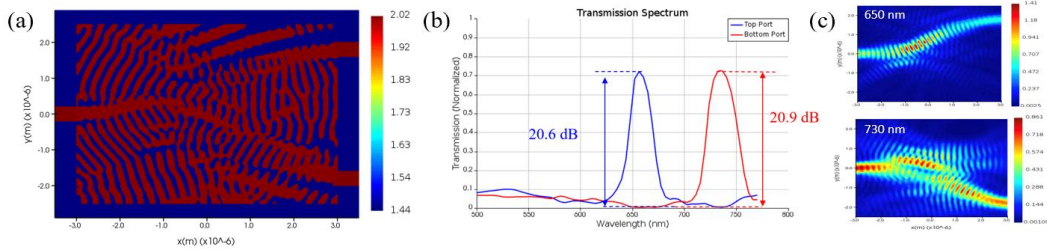


Figure 2: *Inverse-designed wavelength splitter and simulated spectral response.*

(a) Final topology-optimized permittivity distribution of the wavelength splitter obtained through inverse design. (b) Simulated transmission spectra at the output ports showing wavelength-selective routing with ~ 20 dB extinction. (c) Simulated electric field intensity distributions at 650 nm and 730 nm confirming spatial wavelength separation.

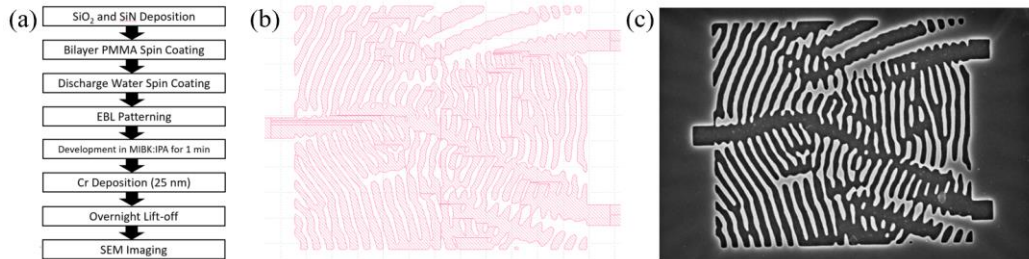


Figure 3: *Inverse-designed wavelength splitter: layout and fabricated structure.*

(a) Schematic of the nanofabrication process sequence. (b) Final binarized layout of the inverse-designed wavelength splitter after applying fabrication constraints. (c) Top-view scanning electron microscope (SEM) image of the fabricated device, showing good agreement with the designed geometry and well-defined nanoscale features.

¹ Piggott, A., Lu, J., Lagoudakis, K. et al. Inverse design and demonstration of a compact and broadband on-chip wavelength demultiplexer. *Nature Photon* 9, 374–377 (2015).

² Jensen, J.S. and Sigmund, O. (2011), Topology optimization for nano-photonics. *Laser & Photon. Rev.*, 5: 308–321.